THE INFLUENCE OF WAVE–FRONT DISLOCATIONS ON THE PHASE CONJUGATION INSTABILITY AT COMPENSATION FOR THERMAL BLOOMING

V.P. Lukin and B.V. Fortes

Institute of Atmospheric Optics,
Siberian Branch of the Russian Academy of Sciences, Tomsk
Received September 27, 1994

The influence of dislocations of an independent reference beam wave front on the efficiency of compensation for thermal blooming occurring along a homogeneous horizontal path is considered in the paper. Some specific features of numerical simulation of adaptive optical systems (AOS) operating in the presence of dislocations in a reference wave are discussed. Correlation between oscillations of corrected beam parameters and periodically occurring dislocations in the reference wave has been found at exact phase conjugation. The oscillating regime has not been observed when simulating AOS with the Hartmann wave–front sensor and using modal algorithm of the phase estimation; in this case eliminating of the quadratic aberrations control from the adaptive contour significantly increases the efficiency of phase correction for thermal blooming.

The problem on reducing the influence of thermal distortions[1] at focusing high–power beams in the atmosphere by introducing forced formation of wave front (WF) at the emitting aperture of an optical system is one of the most interesting applications of the adaptive optics. Known methods of phase control can be divided into three groups: 1) *a priori* (program) control,[2,3] 2) maximization of the focusing criterion,[4] and 3) phase conjugation.[5,6,7]

The present paper is devoted to the application of the phase conjugation (PhC) method to compensation for thermal blooming . This problem has been thoroughly discussed in a series of papers,[5–12] and the results obtained in these papers are indicative of the fact that the phase conjugation technique in application to correction for nonlinear distortions of high–power beams has some specific features including various instabilities. For the case of homogeneous horizontal paths the instability appears as oscillations of the parameters of corrected and reference beams,[7] whereas for vertical paths the small–scale instability is developed[8–12] more strongly.

In the above–mentioned papers the wave front of reference radiation was assumed to be known at all points of the aperture of an adaptive system and can be measured and reproduced with an arbitrary accuracy by means of an ideal wave–front sensor and a corrector. At the same time, in Ref. 13 it was shown that at strong distortions of optical wave the singular points can occur, where the intensity is equal to zero, and the wave front has the singularities in the form of screw dislocations and can be represented by a multisheeted surface. This hypothesis has been confirmed in both laboratory[14] and numerical experiments.[15] As has been noted in the papers devoted to the problem on dislocations, their appearance can significantly affect the operation of adaptive optical systems. However, up to now the investigations are lacking, which could allow one to understand how an adaptive system works under such conditions. The purpose of our paper is the investigation of the influence of dislocations on the efficiency of phase conjugation when compensating for the nonstationary thermal blooming of cw radiation.

MODEL OF PROPAGATION

Propagation of a monochromatic linearly polarized paraxial beam an optically inhomogeneous medium is described by the parabolic wave equation for a slow component of its complex amplitude $\mathbf{E} = \mathbf{e}_E E \exp(i\,\omega\,t - i\,k\,z)$ (Ref. 16)

$$2\,i\,k\,\frac{\partial E}{\partial z} = \nabla_\perp^2 E + k^2(n^2 - n_0^2)\,E\,, \qquad (1)$$

where $k = 2\pi/\lambda$ is the wave number, $\omega = c/\lambda$ is the frequency of electromagnetic oscillations, λ is the wavelength, $\nabla_\perp^2 = \partial^2/\partial x^2 + \partial^2/\partial y^2$ is the transverse Laplacian, $\mathbf{e}_E$ is the polarization vector of the electric field $\mathbf{E}$, and $n(x, y, z)$ is the refractive index. Boundary conditions for the complex amplitude are given as

$$E(\mathbf{r}, 0, t) = A(\mathbf{r}) \exp^{i\varphi(\mathbf{r}, t)}, \qquad \mathbf{r} = (x, y)\,, \qquad (2)$$

where $A(x, y)$ is the amplitude distribution in the beam cross section in the plane of emitting aperture, and φ is its phase. For a continuous Gaussian focused beam considered here we have

$$A(\mathbf{r}) = A_0 \exp\left(-\frac{r^2}{2\,a_0^2}\right); \qquad \varphi(\mathbf{r}, t) = \frac{k\,r^2}{2\,f} + \Phi(\mathbf{r}, t)\,, \qquad (3)$$

where a_0 is the beam radius at the intensity level $1/e$, f is the focal length, $\Phi(\mathbf{r}, t)$ is the phase correction, A_0 is the amplitude on the beam axis.

The field of the refractive index in the high–power beam channel in the isobaric approximation is determined by temperature distribution in its cross section, described by the nonstationary equation of induced heat transfer for the temperature field T (Ref. 1)

$$\frac{\partial T}{\partial t} + \mathbf{V}_\perp \nabla_\perp T = \frac{\alpha}{\rho\,C_p} W(\mathbf{r}, z, t)\,; \qquad (4)$$

$$T(\mathbf{r}, z, t = 0) = T_0\,,$$

0235-6880/95/03 223-07 $02.00

where $W = E\,E^{*}\,8\pi/c\,n_0$ is the beam intensity, $\mathbf{V}_\perp = (V_x, V_y)$ is the transverse component of wind velocity, α is the absorption coefficient, ρ is the density, and C_p is the specific heat at constant pressure.

At small variations of the medium temperature the connection between the temperature and the refractive index can be considered linear: $n - n_0 \approx n_T'(T_0)(T - T_0)$. Assuming $n_0 \approx 1$, after substitution in Eq. (1), we have

$$2\,i\,k\,\frac{\partial E}{\partial z} = \nabla_\perp^2 E + 2\,k^2\,n_T'\,(T - T_0)\,E\,. \qquad (5)$$

Thus, the nonstationary thermal blooming is described by the set of equations (4) and (5) together with the boundary conditions (3).

Both the reflected (or scattered) radiation and radiation from an independent source can serve as the reference wave in AOS. Here we consider only the case of an independent coherent reference beam, being propagated toward the corrected one along the same path. Such an AOS has been created, for example, in the laboratory experiment.[9] Behavior of complex amplitude, $\mathbf{U} = \mathbf{e}_U\,U\,\exp(i\,\omega\,t + i\,k\,z)$, of the reference beam along the path is described by the wave equation

$$-\,2\,i\,k\,\frac{\partial U}{\partial z} = \nabla_\perp^2 U + 2\,k^2\,n_T'\,(T - T_0)\,U\,. \qquad (6)$$

Boundary conditions are set so that in the absence of distortions the complex amplitudes of the high–power and reference beams are conjugated in the plane $z = 0$. For this purpose their complex amplitudes must be conjugated also in the plane $z = f$, i.e.,

$$U(\mathbf{r}, f) = E_0^{*}(\mathbf{r}, f)\,, \qquad (7)$$

where $E_0(\mathbf{r}, f)$ is the solution of Eq. (5) at $T \equiv T_0$ with the boundary conditions (3) at $\Phi \equiv 0$.

For numerical solution of equations describing the propagation of reference and high–power beams we used the splitting method[7,17,18] with a symmetrized splitting operator. In this case all the fields are represented on a three–dimensional grid with the dimensionality $(N_\perp, N_\perp, N_z)$

$$E_{I,J}(z_K) = E(x_I, y_J, z_K) = E(\mathbf{r}_{I,J}, z_K)\,; \qquad (8)$$

$$x_I = h_\perp\,(I - I_0);\; I = 1, 2, \ldots, N_\perp\,;$$

$$y_J = h_\perp\,(J - J_0);\; J = 1, 2, \ldots, N_\perp\,;$$

$$z_K = h_z\left(K - \frac{1}{2}\right);\; K = 1, 2, \ldots, N_z\,,$$

where (I_0, J_0) are the values of indices corresponding to the origin of the coordinates, and $(h_\perp, h_\perp, h_z)$ are the distances between the nodes of the grid. The results of calculations given below were obtained at $N_\perp = 64$, $h_\perp = a_0/8$, $N_z = 16$, and $h_z = f/16$.

PHASE CONJUGATION METHOD

The phase conjugation method is a special case of a more general method of wave front inversion (WFI) based on invertibility of electrodynamics equations. As applied to the used mathematical model, the invertibility of the propagation equation means that if the complex amplitudes E and U are conjugated in the plane $z = 0$, then they are conjugated in the focal plane $z = f$, and *vice versa*:

$$E(\mathbf{r}, 0) = U^{*}(\mathbf{r}, 0) \Leftrightarrow E(\mathbf{r}, f) = U^{*}(\mathbf{r}, f)\,. \qquad (9)$$

Owing to the technical problems occurring in the wave amplitude control, in AOS one usually restricts oneself to the phase control, that is, uses the phase conjugation method

$$\mathrm{Arg}\,(E(\mathbf{r}, z=0)) = \mathrm{Arg}\,(U^{*}(\mathbf{r}, z=0)) - \mathrm{Arg}\,(U(\mathbf{r}, z=0))\,. \qquad (10)$$

If the distributions of amplitude modules of the reference and corrected fields are close

$$A(\mathbf{r}) = |E(\mathbf{r}, 0)| \approx |U(\mathbf{r}, 0)| \qquad (11)$$

(or they differ by a constant factor), then one can look forward to high efficiency of such a purely phase control. The boundary condition for a corrected beam takes the form

$$E(\mathbf{r}, 0) = A(\mathbf{r})\,\exp\,(-\,i\,\mathrm{Arg}\,(U(\mathbf{r}, 0))) \qquad (12)$$

or

$$E(\mathbf{r}, 0) = A(\mathbf{r})\,\exp\,(-\,i\,\arg\,(U(\mathbf{r}, 0)))\,. \qquad (13)$$

Mathematical formulation of the PhC method (12) has two peculiarities. First, the argument of the complex number is determined accurate to $2\pi m$, $m = \pm 1, \pm 2, \ldots$; second, the argument of zero complex number is undefined.

If in the case of numerical simulation of AOS the corrected field is determined through the principal value of the argument of the reference wave complex amplitude (13) then the first peculiarity is inessential. However, in simulating the wave–front corrector to calculate the approximation of the required surface we need for untruncated phase while the principal value of the argument is limited by the range $[-\pi, \pi]$. To obtain the untruncated phase, the operation of phase joining should be performed. It is common practice in this case to calculate the phase differences and then the problem on the function reconstruction is solved on the basis of the values of its first differences in two directions. At numerical simulation the phase difference at two adjacent nodes of the grid is determined as follows:

$$\Delta_{I,J}^{x} = \mathrm{Arg}\,(U_{I+1,J}) - \mathrm{Arg}\,(U_{I,J}) = \arg\,(U_{I+1,J}) + 2\pi\,m_{I+1,J} -$$

$$-\,\arg\,(U_{I,J}) - 2\pi\,m_{I,J} = \arg\,(U_{I+1,J}) - \arg\,(U_{I,J}) + 2\pi\,k_{I,J}^{x}\,,$$

$$|k_{I,J}^{x}| \le 1 \qquad (14)$$

and similarly for $\Delta_{I,J}^{y}$. The values of $k_{I,J}^{x}$, $k_{I,J}^{y} \in \{-1, 0, 1\}$ are determined from the conditions $|\Delta_{I,J}^{x}| \le \pi$ and $|\Delta_{I,J}^{y}| \le \pi$ (Ref. 15). Similarly the phase differences can be determined as

$$\Delta_{I,J}^{x} = \arg\,(U_{I+1,J}\,U_{I,J}^{*})\,; \qquad (15)$$

$$\Delta_{I,J}^{y} = \arg\,(U_{I,J+1}\,U_{I,J}^{*})\,.$$

The problem on reconstructing untruncated phase from its differences calculated from the complex amplitude at the nodes of the reference grid is mathematically equivalent to the problem on phase reconstruction from phase differences obtained from the data of an interferometer sensor or estimated by the local phase tilt measured using a Hartmann sensor. Since the number of differences is twice as large as the number of points, where the phase value must be obtained, such a problem is excessive and some additional conditions are usually fomulated, namely, minimizing of squared discrepancy[19]

$$\sum_{I,J}[(\phi_{I+1,J}-\phi_{I,J})-\Delta^x_{I,J}]^2+[(\phi_{I,J+1}-\phi_{I,J})-\Delta^y_{I,J}]^2\to\min \quad (16)$$

or minimizing of integral variance of the estimation error[20]

$$<\sum_{I,J}(\phi_{I+1,J}-\hat{\phi}_{I,J})^2>\to\min\ . \quad (17)$$

Here the statistical averaging is denoted by angular brackets, $\phi_{I,J}$ is the sought estimate of the phase, and $\hat{\phi}_{I,J}$ is its exact value. In both cases the problem is reduced to the solution of a set of linear equations of the following form:

$$\phi_{I+1,J}+\phi_{I-1,J}+\phi_{I,J+1}+\phi_{I,J-1}-4\phi_{I,J}=\Delta^x_{I,J}+\Delta^y_{I,J}-\Delta^x_{I-1,J}-$$

$$-\Delta^y_{I,J-1}\ . \quad (18)$$

When the differences are set on a uniform grid, we can use for solution of this problem the method of discrete Fourier transform (DFT) and the fast Fourier transform (FFT) algorithm[21,22] if the number of grid nodes satisfies appropriate requirements. Solution of the set of equations (18) reconstructs the argument of complex amplitude accurate to a constant

$$\mathrm{Arg}(U_{I,J})=\phi_{I,J}+C\ ; \quad (19)$$

$$U_{I,J}=|U_{I,J}|\ \exp\,[i\,(\phi_{I,J}+C)]$$

and exactly corresponds to the initial values of differences

$$\phi_{I+1,J}-\phi_{I,J}=\Delta^x_{I,J},\qquad \phi_{I,J+1}-\phi_{I,J}=\Delta^y_{I,J}\ , \quad (20)$$

if the field U has no zero values in the region considered.

SCREW DISLOCATIONS OF THE WAVE FRONT

At the points where the complex amplitude (CA) of an optical wave is exactly equal to zero, its argument is uncertain. If the point under consideration is the intersection of lines, where the real and imaginary parts of CA change sign, this point is the center of screw dislocation of the wave front. The existence of such dislocations was predicted theoretically[13] and supported by the results of laboratory[14] and numerical[15] experiments.

Let us consider the vector field $\mathbf{g}=(g_x\,,\,g_y)$ defined as follows:

$$g_x(x,y)=\lim_{\Delta x\to 0}\frac{1}{\Delta x}\arg\left[U\left(x+\frac{\Delta x}{2},\,y\right)U^*\left(x-\frac{\Delta x}{2},y\right)\right]; \quad (21)$$

$$g_y(x,y)=\lim_{\Delta y\to 0}\frac{1}{\Delta y}\arg\left[U\left(x,y+\frac{\Delta y}{2}\right)U^*\left(x,\,y-\frac{\Delta y}{2}\right)\right].$$

The field $\mathbf{g}(\mathbf{r})$ is, by definition, the gradient of the optical wave phase, and it is so if $U(\mathbf{r})$ vanishes nowhere

$$|U(\mathbf{r})|\neq 0\Rightarrow\mathbf{g}=\nabla\ \mathrm{Arg}\ (U(\mathbf{r}))\ . \quad (22)$$

In presence of dislocations, the field $\mathbf{g}$ has singularities and ceases to be a purely potential field, and the contour integral

$$\oint_C \mathbf{g}\,d\,\mathbf{r}=\pm\,2\pi\,(N_+-N_-) \quad (23)$$

is determined by the number of dislocations inside this contour and twisted in positive, N_+, and negative, N_-, directions.[13,14] In this case the phase difference expressed in terms of the contour integral

$$\phi(\mathbf{r}_2)-\phi(\mathbf{r}_1)=\int_{\mathbf{r}_1}^{\mathbf{r}_2}\mathbf{g}\,d\,\mathbf{r} \quad (24)$$

depends on the path of integration, and the equation

$$\nabla\,\phi=\mathbf{g} \quad (25)$$

has no solution.

It is well known that any vector field $\mathbf{g}$ can be represented as a sum of irrotational $\mathbf{g}_1$ and solenoidal $\mathbf{g}_2$ components

$$\mathbf{g}=\mathbf{g}_1+\mathbf{g}_2\ , \quad (26)$$

the solenoidal component can be here excluded by the use of the divergence operator[22,23,24] so that the solution of the Poisson equation

$$\nabla^2\,\phi=\mathrm{div}\,\mathbf{g}=\mathrm{div}\,\mathbf{g}_1 \quad (27)$$

corresponds to the potential part of the reference field $\mathbf{g}$

$$\nabla\,\phi=\mathbf{g}_1\ . \quad (28)$$

Since the set of linear equations (18) is the finite–difference representation of the Poisson equation (27), the algorithm of reconstruction, solving the set of linear equations (18), filters the wave–front dislocations, thus smoothing out the estimate of the optical wave phase.

A number of the results on numerical simulation of phase conjugation has been obtained based on the boundary condition of the exact phase conjugation

$$E_{I,J}(0)=A_{I,J}\,\exp\,[i\,\arg\,(U_{I,J}(0))]\ . \quad (29)$$

As a rule, dislocations do not fall accurately on the grid nodes, and the boundary condition (29) is correct. However, the corresponding analytical boundary condition

$$E(\mathbf{r},\,0)=A(\mathbf{r})\,\exp\,[i\,\arg\,(U(\mathbf{r},\,0))] \quad (30)$$

is uncertain at the points where $U(\mathbf{r},\,0)=0$. When $A(\mathbf{r})\neq 0$, at the same points the continuity of the field $E(\mathbf{r},\,0)$ breaks down, and it becomes nondifferentiable. Although the grid boundary condition (29) can also be considered to be a result of application of a corrector with the element size equal to the distance between the grid nodes, care must be exercised in the interpretation of the results of numerical experiment since the corresponding analytical boundary condition (30) is incorrect.

To better understand how the specific boundary conditions of the type (29) work at the appearance of dislocations in the reference beam, we have performed a numerical experiment in which we have calculated diffraction of the beam with the Gaussian intensity profile under the boundary condition of the form

$$E(\mathbf{r}, 0) = A(\mathbf{r}) \exp [i \arg (x + i\, y))] . \quad (31)$$

As is evident from Ref. 13, the field

$$U(\mathbf{r}, z) = e^{i\gamma} (B_x\, x + i\, B_y\, y) , \quad (32)$$

where γ, B_x, and B_y are real constants, satisfies the parabolic wave equation in vacuum and has its dislocation at the origin of coordinates. Thus, the boundary condition (31) describes the field with the dislocation at the point $\mathbf{r} = 0$. In this case its intensity is different from zero everywhere.

Figure 1 shows intensity distribution over the cross section of such a beam for different values of $z' = z/z_d$, where $z_d = ka_0^2$ is the diffraction length. At the center of the beam the intensity dip occurs reaching practically zero value at $z' = 0.1$. Similar effect is observed at compensation for thermal blooming when a dislocation appears in the reference beam.

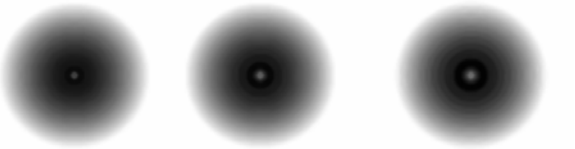

FIG. 1. Beam cross sections at the diffraction of a beam under boundary conditions (31) in vacuum. From left to right: $z' = 0.03$, $z' = 0.06$, *and* $z' = 0.09$.

PHASE CORRECTION FOR THERMAL BLOOMING

We have conducted two types of numerical experiments on application of the phase conjugation method to correction for thermal blooming. In one experiment we used for the corrected beam the boundary condition of exact conjugation (30), and in the other case – the boundary condition (3). The phase correction $\Phi(\mathbf{r}, t)$ was obtained as a result of simulation of the Hartmann sensor[25] and subsequent modal estimation of the reference beam phase.[26,27]

In both cases we have simulated a "high–speed" adaptive system, focusing the Ganssian beam on a target plane, at the distance $f = \frac{1}{\sqrt{10}}\, z_d$. At diffraction the intensity at focus of such an optical system in vacuum is 10 times as large as the axial intensity in the emitting aperture. In the focal plane we recorded the peak intensity $W_{\max}$ and the radiant flux P through a circle of a radius $a_f = a_0 f/z_d$ equal to the radius of the undistorted beam at the intensity level of $1/e$. About 63% of the undistorted beam power is within this circle. Simultaneously we recorded the appearance and coordinates of dislocations of the reference beam wave front in the plane $z = 0$. For this purpose at each node of the grid within the circle of radius $2a_0$ we calculated the value

$$\Sigma_{I, J} = \Delta^x_{I, J} + \Delta^y_{I+1, J} - \Delta^x_{I, J+1} - \Delta^y_{I, J} \quad (33)$$

corresponding to the integral (23) over the contour shaped by four adjacent nodes of the grid. For the majority of nodes $\Sigma_{I, J} \cong 0$ accurate to the errors of arithmetical operations. The nodes, for which $\Sigma_{I, J} \cong \pm 2\pi$, correspond to the contours containing one or more dislocations. The case when $\Sigma_{I, J} > \pi$, we consider to be indicative of a dislocation, to whose coordinates are assumed to be at the contour center (x_d, y_d)

$$x_d = h_\perp (I + \tfrac{1}{2} - I_0), \qquad y_d = h_\perp (J + \tfrac{1}{2} - J_0) . \quad (34)$$

Of course, such a method does not permit detection of a pair of dislocations with different signs falling into the contour considered, but in this case they do not affect the solution of the propagation problem.

Let us consider the results of simulation of the exact phase conjugation. Figure 2 presents the curves indicating the dependence of peak intensity $W_{\max}$ and the coordinate of dislocation x_d on the time t, normalized as follows[7]:

$$t' = \frac{t}{\tau_\nu}, \ \tau_\nu = \frac{2\, a_0}{V}; \ W' = W \frac{2\, k^2\, \alpha\, n'_T\, a_0^3}{\rho\, C_p\, V_\perp\, n_0};$$

$$P' = P \frac{2\, k^2\, \alpha\, n'_T\, a_0}{\rho\, C_p\, V_\perp\, n_0}; \qquad x'_d = \frac{x_d}{a_0} \quad (35)$$

(below the primes at normalized values are omitted). The plots are given for two values of axial intensity of the initial beam: $W_0 = 16$ and $W_0 = 24$.

At the beam intensity $W_0 = 16$ (curve *1*) the dislocations do not appear, and the beam parameters become stationary. With the increase of beam intensity up to 24 we observe the intensity fluctuations (curve *2*) followed by periodic appearance of dislocations in the reference beam (curve *3*). Dislocations appear close to the axis of the optical system and travel along the direction coinciding with the wind direction $\mathbf{V} = (V_x, 0)$, $V_x > 0$, until they go out from the zone $x_d^2 + y_d^2 \le (2a_0)^2$ recorded. The increase of intensity to 32 results in the fact that a new pair of dislocations appears before the preceding pair goes out from the zone.

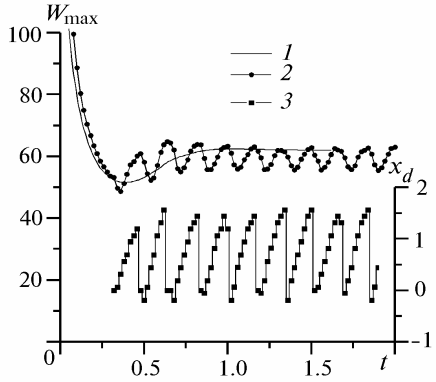

FIG. 2. Dynamics of the peak intensity $W_{\max}(t)$ *of a corrected beam in the focal plane at the beam initial intensity* $W_0 = 16$ *(1),* 24 *(2), and the coordinate of the reference beam dislocation* $x_d(t)$ *at* $W_0 = 24$ *(3).*

Figure 3 shows typical intensity distribution of a corrected beam in the cross section $z = f/32$. Two intensity dips, travelling leeward in the beam, correspond to two dislocations in the phase of the reference beam.

To understand the mechanism of oscillations, shown in Fig. 2, the coordinate of the cross section $z_{\max}$ was recorded, at which the peak intensity of a corrected beam is maximum (the position of beam caustic). Figure 4 shows time dependence of the position of the beam caustic $z_{\max}$ and peak intensity in it. At the intensity $W_0 = 16$ the beam caustic gradually shifts to the emitting aperture and its position is

stabilized at the point $z_{max} \approx 0.85f$. At $W_0 = 24$ the caustic shifts closer to the emitting aperture and its position oscillates near the point $z_{max} \approx 0.4f$ with the amplitude of the order of $\Delta z_{max} \approx 0.15f$. At the same time, the intensity in the caustic strongly exceeds the initial intensity of the beam. The period of oscillations of the caustic position coincides with the period of the dislocation appearance.

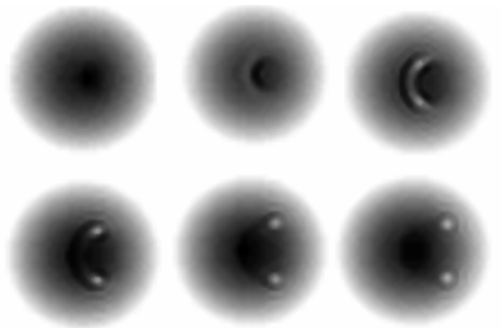

FIG. 3. Intensity distribution of a corrected beam in the cross section $z = f/32$ with the wave–front dislocations appearing in the reference beam, $W_0 = 24$. The upper row: $t = 0.50$, 0.52, and 0.54; the lower row: $t = 0.56$, 0.58, and 0.60.

This effect can be interpreted as a manifestation of the positive feedback between the adaptive system and the thermal lens. At the initial stage of heating $t \le \tau_V$ the main contribution to distortions comes due to defocusing. Its compensation results in an additional focusing of a high–power beam and its caustic shifts to the source. The caustic becomes narrower, and the beam intensity in it increases that leads to the temperature increase in the beam caustic and to strengthening of the defocusing effect of the thermal lens. This in turn results in a subsequent shift of the caustic, and so on.

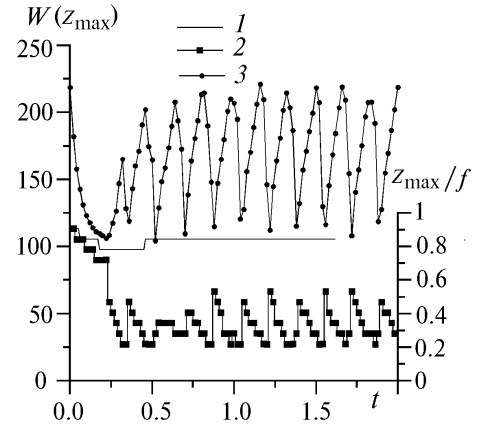

FIG. 4. Dynamics of the caustic position of a high–power beam, $z_{max}(t)$, at $W_0 = 16$ (1) and 24 (2), and peak intensity in the caustic for $W_0 = 24$ (3).

The thermal lens shift towards the emitting aperture decreases "the feedback coefficient". In the limiting case when the thermal lens strength is concentrated close to the AOS aperture and the additional focusing, contributed by the AOS, is compensated for by the defocusing thermal lens, we do not observe any subsequent increase in defocusing of the reference beam and in focusing of the high–power beam.

If the distortions in the high–power beam caustic achieve the value sufficient for appearance of a dislocation in the reference beam, the information on the defocusing introduced by the thermal lens is erased without entering into the adaptive system, and the high–power beam focusing decreases whereas its caustic shifts towards the target. As a result, the thermal lens, being the cause of occurrence of dislocations, cools and some time later the lens is cooled down to the state when dislocations disappear and the feedback is restored. Then the whole cycle is repeated and the system develops into the oscillatory state typical for nonlinear systems with a feedback.

At the next stage of the work, an AOS with the Hartmann sensor, consisting of 16 subapertures arranged in four rows, is simulated. Four corner subapertures are not taken into account, and local tilts are estimated only in 12 subapertures (Fig. 5). The size of the sensor aperture $D = 4a_0$ corresponds to the beam diameter at the intensity level of $1/e^2$. The reference beam coming to the sensor is assumed to be passed through a correcting and a focusing optical systems

$$U(\mathbf{r}, 0, t + \Delta t) \exp\left(i \frac{k r^2}{2 f} + i \Phi(\mathbf{r}, t) \right) . \qquad (36)$$

The phase correction is determined as a sum of Zernike polynomials Z_l

$$\Phi(\mathbf{r}, 0) = 0 ; \qquad (37)$$

$$\Phi(\mathbf{r}, t + \Delta t) = \Phi(\mathbf{r}, t) + \Delta\Phi ;$$

$$\Delta\Phi = \sum_{l=2}^{15} c_l (t + \Delta t) Z_l \left(\frac{\mathbf{r}}{2 a_0} \right)$$

with the weighing factors c_l obtained by the modal estimation of the phase[25,26,27] on the circle inscribed in the sensor aperture.

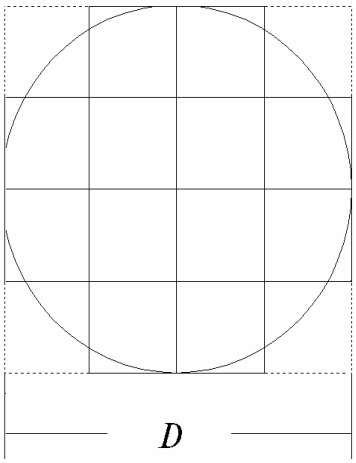

FIG. 5. Configuration of the wave–front sensor.

Figure 6 shows the dynamics of the peak intensity in the focal plane on a target at three values of the initial beam intensity. In all the three cases we have no oscillations, i.e., the application of the Hartmann sensor with modal estimate damps the oscillations or, at least, increases the threshold of their appearance. Nevertheless, the dislocations in the reference beam could appear. It turned out that in the focus of the sensor subaperture, into which the dislocation falls, two focal spots are observed, each having the diffraction size (Fig. 7). In contrast to AOS

with the exact phase conjugation, the positions of dislocations are relatively stable.

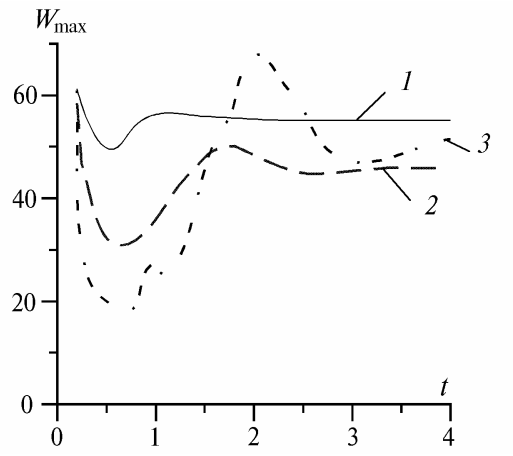

FIG. 6. Dynamics of peak intensity $W_{max}(t)$ in the AOS focus with the Hartmann sensor at W_0 = 16 (1), 32 (2), and 64 (3).

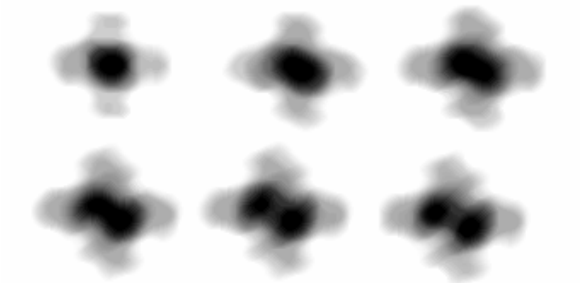

FIG. 7. Dynamics of the intensity distribution in the subaperture focus of the Hartmann sensor with dislocation appearing in the reference beam.

Since the phase correction is now determined by the weighted sum of the Zernike polynomials, it becomes possible to control directly the aberration spectrum of the phase correction. The above considerations enable us to assume that the positive feedback between the adaptive system and the thermal lens is closed mainly by the control of squared aberrations. Furthermore such a feedback affects negatively the correction efficiency. Besides, it is known that at thermal blooming the optimal focal length is longer[17] than in vacuum while the adaptive correction decreases the focal length of the system, compensating for the thermal lens effect.

The first step that we can propose for decreasing the harmful influence of this effect is the complete exclusion of the focusing control

$$\Delta\Phi = \sum_{l=2}^{15} (1 - \delta_{l,4}) c_l (t + \Delta t)\, Z_l\left(\frac{\mathbf{r}}{2\, a_0}\right),$$

$$\delta_{lm} = \begin{cases} 0, & l \neq m, \\ 1, & l = m. \end{cases} \qquad (38)$$

It turned out that the exclusion of the control over astigmatism

$$\Delta\Phi = \sum_{l=2}^{15} (1 - \delta_{l,4})\,(1 - \delta_{l,5})\,(1 - \delta_{l,6})\, c_l\, Z_l \qquad (39)$$

provides for an additional increase in the correction efficiency. Since in addition to squared aberrations the tilt and coma also contribute greatly, the correction by Eq. (39) results mainly in a better beam pointing and straightening of a characteristic "sickle" owing to coma.

Figure 8 shows the steady state values of the parameters of a corrected beam depending on the initial intensity when correcting by the formula (37) (curve *1*) and by formula (39) (curve *2*), that is, without control over the total beam focusing and astigmatism. Curve *3* in this figure corresponds to the exact phase conjugation (the boundary condition (29)), and curve *4* corresponds to the system without a correction. The data for the exact phase conjugation are obtained by averaging over time corresponding instantaneous values.

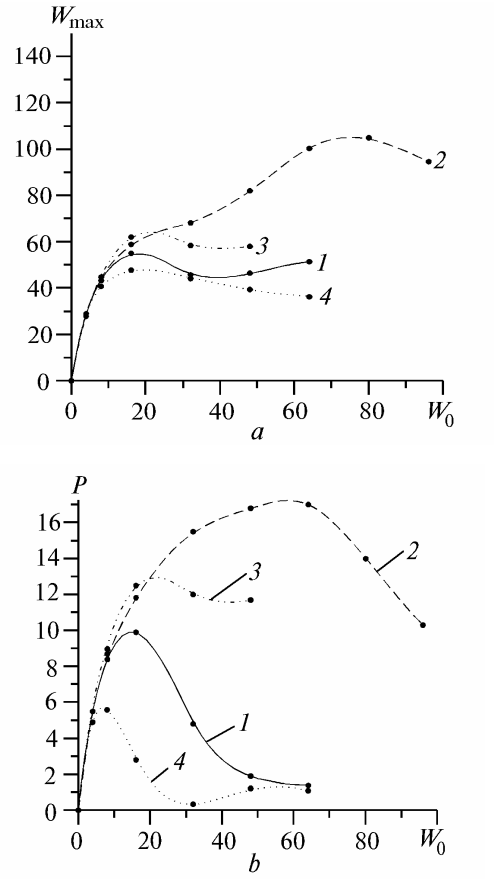

FIG. 8. Dependence of the peak intensity W_{max} (a) and radiant flux at the target P(b) on the beam initial intensity W_0 for different versions of AOS: AOS with the Hartmann sensor (37) (1), AOS with the Hartmann sensor (39) (2), exact PhC (3), and without a correction (4).

It is known that the efficiency of correction by the formula (37) is somewhat lower than the efficiency of the exact phase conjugation while the correction by the formula (39) (without control over squared aberrations) is more effective than the exact phase conjugation starting from the power, at which the dislocations and oscillatory state occur ($W_0 \approx 20$–24). Together with the optimization of the beam initial intensity the correction by the formula (39) gives more than twofold gain in the peak intensity in the focal plane as compared to the system without a correction and approximately 1.5–fold gain as

compared to the exact phase conjugation, whereas the gain in power P is 3– and 1.5–fold, respectively.

Of course, the exclusion of control over squared aberrations will give the gain not in all situations. For the beams with the nongaussian profile of intensity and for vertical paths or for beam scanning the results may be different. In particular, for the vertical paths the small–scale instability is more typical and for suppressing it one must exclude the small–scale part of the reference beam phase.[8]

CONCLUSION

We have considered the problem on compensation for nonstationary thermal blooming by the phase conjugation method. Analysis of the numerical experiment has shown that the appearance of sustained free oscillation in the adaptive system is connected with the occurrence of dislocations in the reference beam.

The use of a Hartmann sensor with low spatial resolution and modal estimation of the phase results in smoothing of the phase estimate and damps the AOS oscillations.

Adaptive compensation for defocusing and astigmatism results in the shift of the beam caustic towards the source and in the appearance of strong thermal lens. Exclusion of the square aberrations control weakens this effect and increases the efficiency of correction for thermal blooming along a homogeneous path.

REFERENCES

1. D.K. Smith, IEEE **65**, No. 12, 59–103 (1977).
2. L.C. Bradley and J. Herrmann, Appl. Opt. **13**, No. 2, 331–334 (1974).
3. J.A. Fleck and J.R. Morris, Appl. Opt. **17**, No. 16, 2575–2579 (1978).
4. C.A. Primmerman and D.G. Fouche, Appl. Opt. **15**, No. 4, 990–995 (1976).
5. J.Herrmann, J. Opt. Soc. Am. **67**, No. 3, 290–295 (1977).
6. M.A. Vorontsov, Kvant. Elektron. **6**, No. 10, 2078–2083 (1979).
7. V.E. Zuev, P.A. Konyaev, and V.P. Lukin, Izv. Vyssh. Uchebn. Zaved. SSSR, Ser. Fizika **28**, No. 11, 6–29 (1985).
8. V.L. Dmitriev, A.A. Mishukova, V.P. Lukin, and V.V. Sychev, Atm. Opt. **3**. No. 12, 1149–1151 (1990).
9. B.Johnson and C. Primmerman, Opt. Lett. **14**, No. 12, 639–641 (1989).
10. T.J. Karr, Proc. SPIE **1060**, 120–128 (1989).
11. J.F. Schonfeld, J. Opt. Soc. Am. B **9**, No. 10, 1803–1812 (1992).
12. P.A. Konyaev, Atmos. Oceanic Opt. **5**, 814–818 (1992).
13. N.B. Baranova and B.Ya. Zel'dovich, Zh. Eksp. Teor. Fiz. **80**, 1789–1797 (1981).
14. N.B. Baranova, A.V. Mamaev, N.F. Pilipetsky, V.V. Shkunov, and B.Ya. Zel'dovich, J. Opt. Soc. Am. **73**, No. 5, 525–528 (1983).
15. D.L. Fried and J.L. Vaughn, Appl. Opt. **31**, No. 15, 2865–2882 (1992).
16. J. Walsh and P. Ulrich, in: *Laser Beam Propagation through the Atmosphere*, ed. by J.W. Strohben (Springer–Verlag, Berlin–Heidelberg–New York, 1976).
17. J.A. Fleck, J.R. Morris, and M.D. Feit, Appl. Phys. **10**, No. 1, 129–139 (1976).
18. G.I. Marchuk, *Methods of Computational Mathematics* (Nauka, Moscow, 1980), 535 pp.
19. D.L. Fried, J. Opt. Soc. Am. **67**,No. 3, 370–375 (1977).
20. R.H. Hudgin, J. Opt. Soc. Am. **67**, No. 3, 375–378 (1977).
21. K. Freischlad and C.L. Koliopoulos, Proc. SPIE **551**, 74–80 (1985).
22. A.N. Bogaturov, Izv. Vyssh. Uchebn. Zaved. SSSR, Ser. Fizika **28**, No. 11, 86–95 (1985).
23. J. Herrmann, J. Opt. Soc. Am. **70**, No. 1, 28–35 (1980).
24. R.J. Noll, J. Opt. Soc. Am. **68**, No. 1, 139–140 (1978).
25. V.P. Lukin, N.N. Maier, and B.V. Fortes, Atmos. Oceanic Opt. **5**. No. 12, 801–807 (1992).
26. R. Cubalchini, J. Opt. Soc. Am. **69**, No. 7, 972–977 (1979).
27. J. Herrmann, J. Opt. Soc. Am. **71**, No. 8, 989–992 (1981).
28. D.C. Ghiglia and L.A. Romero, J. Opt. Soc. Am. **11**, No. 1, 107–117 (1994).